Materials and Methods

9. Plant growth procedure

B73 inbred maize line seeds (supplied by Pannar Seed (Pty)Ltd, South Africa) were grown under two conditions: sterile culture on *in vitro* media in doubled magenta boxes, and in soil. For the former, seeds were first surface-sterilised using a sequential ethanol-bleach washing step which has been shown to significantly lower contamination in media (Sauer and Burroughs, 1986). These were then inserted into sucrose-fortified MS salt medium: 2.16g/L Murashige and Skoog basal salt mixture (Sigma-Aldrich, Schnelldorf, Germany); 12g/l Bacteriological agar (Merck, Cape Town, South Africa); 30g/l sucrose. The seeds were germinated and grown under controlled conditions in a phytotron (16 hours per day, 330uE, 25°C) for one month (figure 2).

Figure 2. An example of a media-grown maize plant, removed from it's doubled-magenta box.

For the latter, plants were grown in sand-coir soil pots (supplied by University of Pretoria Experimental Farm) for 8 weeks (V4 stage) under either artificial (optimisation experiments) or natural (validation experiments) light. Artificial light conditions were provided by the same facility as the media-grown plants (16 hours per day, 330uE, 25°C). Watering was performed every second day, with supplemental nutrients (Multifeed® water soluble fertilizer; Wenkem SA (Pty)Ltd, Pretoria, South Africa) being applied once a week

(see figure 3).

Figure 3. Sand-coir grown maize plants, grown to V4 stage.

10. Sample preparation

For each trial (consisting of 6 bombardments), five plants were selected and harvested using the procedure laid out in Kirienko et al (2012). Plants were cut transversely through the stalk at around the level of the first visible node (figure 4). These were then placed in distilled water before being stripped of emergent leaves. The non-emergent leaves were sorted into three categories (central whorl, inner and outer) based on their depth in the leaf whorl arrangement (figure 5), with the required category being reserved for final dissection. The final samples consisted of these leaves, cut into sections 0-3cm and 3-6cm from the ligule (figure 6), and then split from the leaf midrib.

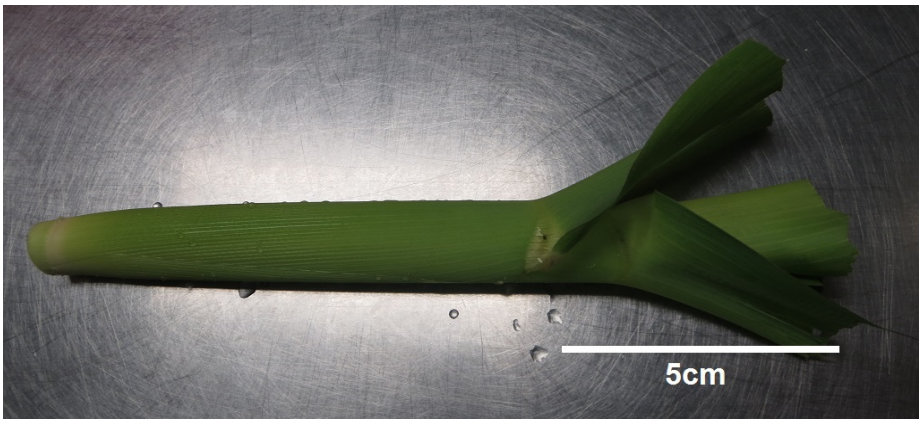

Figure 4. Maize leaf sample prior to dissection.

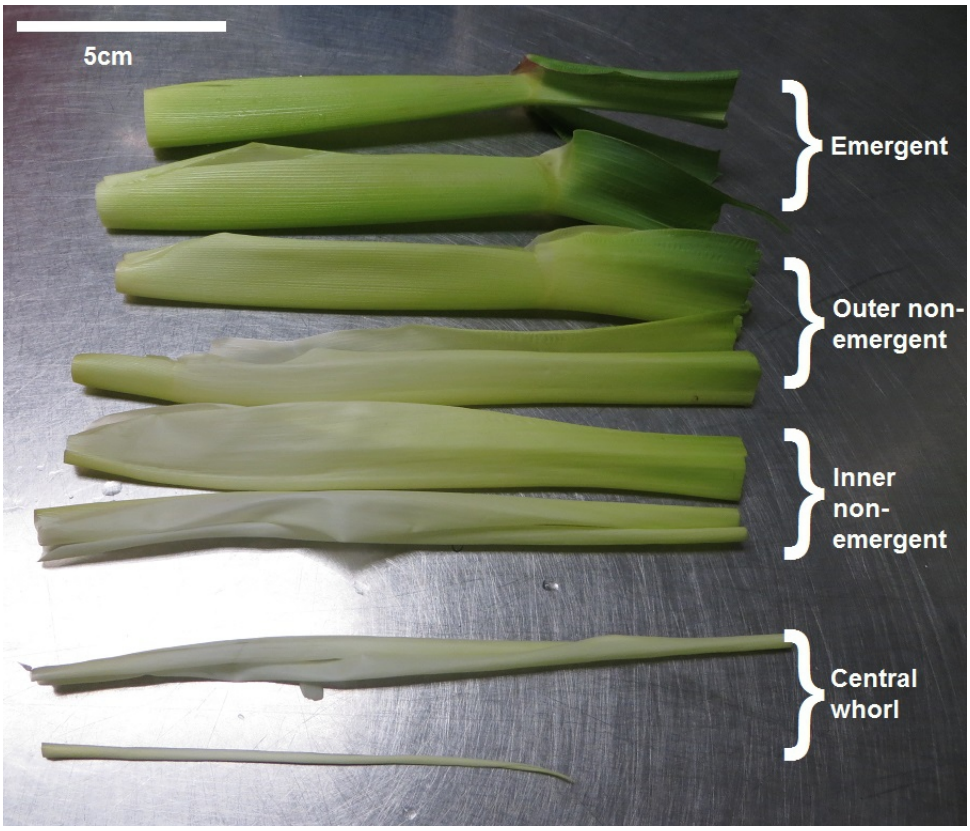

Figure 5. Leaf sample selection after dissection. Samples are named according to the scheme used in Kirienko et al, 2012.

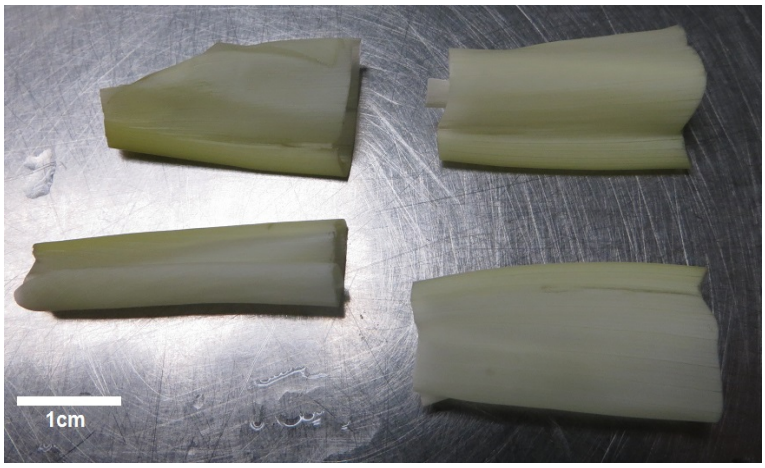

Figure 6. Selected samples after separation along leaf axis from ligule. From left to right: 0-3cm leaf samples, 3-6cm ligule samples. Samples are split from leaf midrib prior to placement on plates.

Once processed, the leaf samples were pooled before being transferred to wetted filter paper wicks (4ml sterile dH_2O per wick) placed inside 90mm petri dishes. Samples were arranged adaxial side up, with three samples per plate being used to cover the bombarded area (figure 7).

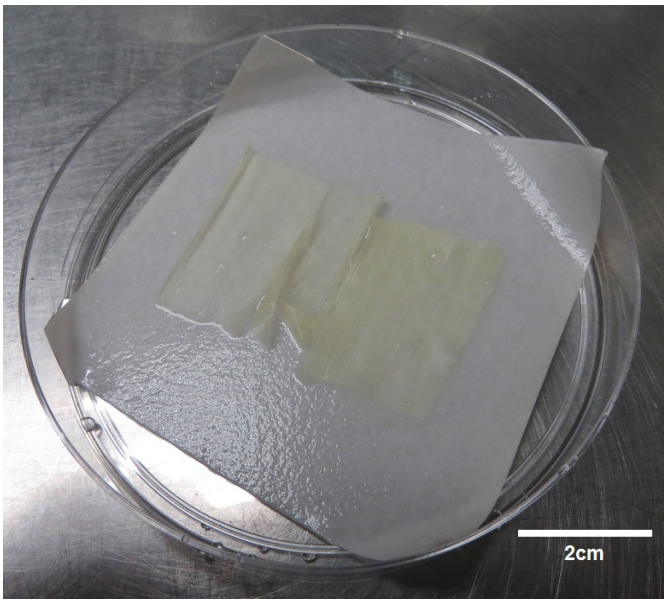

Figure 7. Processed samples immediately prior to bombardment.

11. DNA binding protocol

Microparticle preparation and DNA binding protocols were taken from literature (Frame et al, 2000), using 1.1um M17 tungsten microparticles (Bio-Rad, Hercules, United States of America) as carriers. Microcarriers were prepared by weighing out 10X the final amounts into an Eppendorf tube. Thereafter the microcarriers were washed with 70% ethanol, spun down, rinsed with sterile, distilled water, spun down again, re-suspended in the same and separated into 100µl, 1X aliquots. The aliquots were subsequently placed in long-term storage at -20°C.

When needed, the prepared microcarrier samples were taken from cold storage, thawed, and ground with a sterile blue tip and sonicated to disaggregate the particles (which tend to clump together). The tubes were then finger vortexed before being spun down for 15 seconds at 6000rpm in a micro-centrifuge. Excess liquid was pipetted off before the addition of the pAHC25 DNA construct (figure 8) at a concentration of 3ug/µl. The reporter gene component of the construct consisted of a ubiquitin promoter, intron, *Uid A* GUS coding sequence and NOS terminator region.

Thereafter, 25µl of 2.5M $CaCl_2$ (Merck, Cape Town, South Africa) and 10µl of 0.1M spermidine (Sigma-Aldrich, Schnelldorf, Germany) were added in sequence, with vigorous mixing (either mechanical or finger vortexing) between each addition. The mixture was then vortexed mechanically for five minutes before standing for another five minutes.

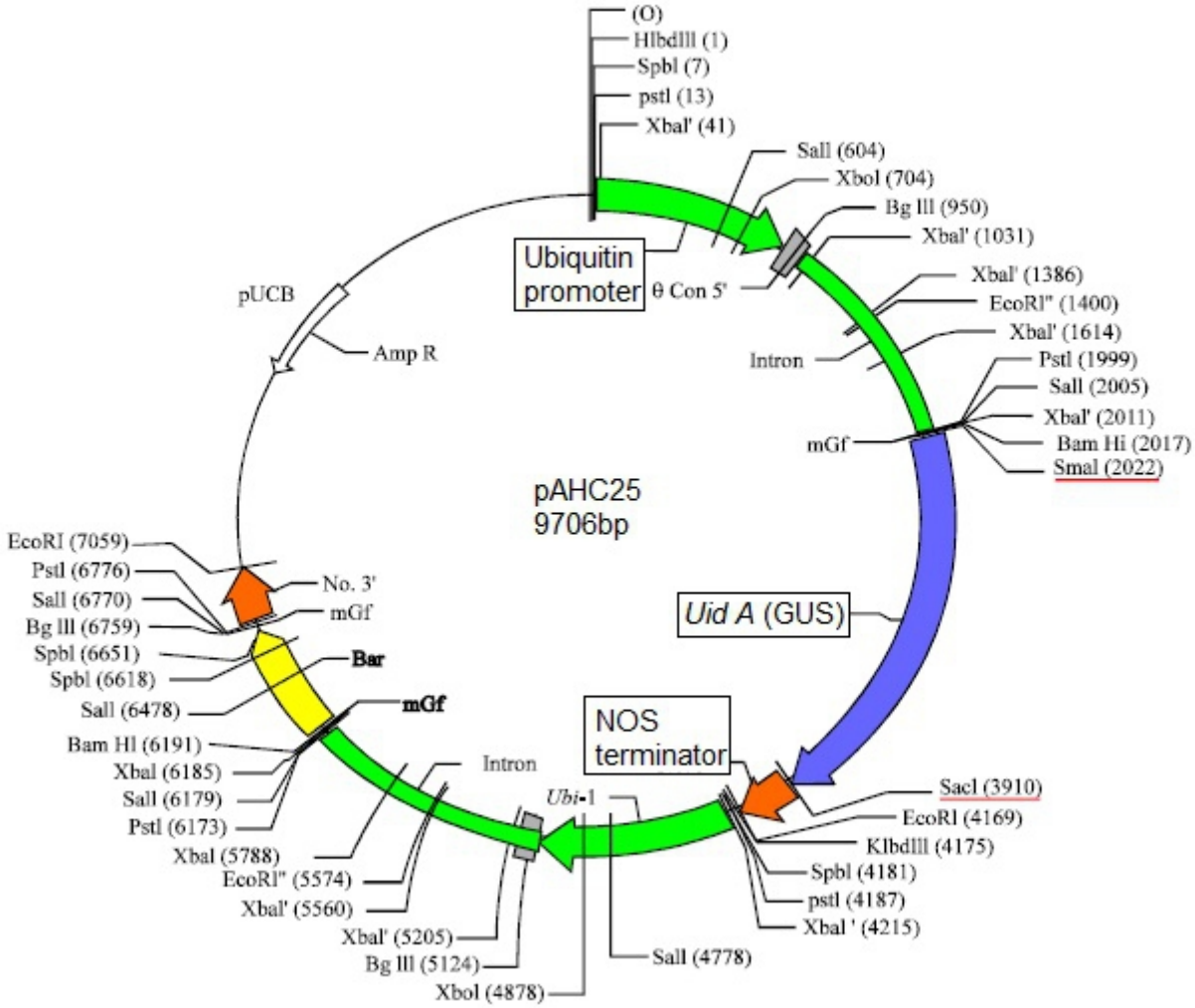

Figure 8. pAHC25 plasmid map (modified from image taken from Kader et al, 2012). Outlined labels indicate reporter gene construct components.

After standing, the samples were spun down for 15 seconds at 6000rpm and the supernatant pipetted off. The samples were then washed in 125µl, ice-cold, analysis-grade 100% ethanol (Merck, South Africa) before being spun down again. During the washing step, gentle grinding with a pipette tip was done to disaggregate the clumps that formed, with hard finger vortexing to separate the particles into a sandy-looking slurry. After spinning down, the supernatant was again removed and 60µl of analysis-grade ethanol was added. The samples were then placed on a mechanical vortex until needed for bombardment.

Each binding step produced enough microcarriers for three bombardments. Negative controls for bombardments consisted of a mock bombardment using the same binding procedure but substituting sterile water for construct DNA.

12. Microprojectile bombardment

Prepared leaf sample plates were placed in a laminar flow hood for bombardment using a Biorad PDS-1000He gene gun (figure 9). The plastic macrocarriers (plastic discs about 25mm in diameter) for the device were fitted into their holders and loaded with microcarriers (15µl of microcarrier mixture per macrocarrier, due to evaporation of some of the liquid) before being left under the flow to air dry. Care was taken to ensure equal distribution of microcarriers, with samples being kept on low vortex prior to loading.

Figure 9. Bio-Rad PDS 1000/He biolistic device. Retrieved 2 March, 2014, from Bio-Rad Life Science Research: http://www.bio-rad.com/ja-jp/product/pds-1000-he-hepta-systems

Once dried, the device was assembled for firing and samples were bombarded. This was done in stages, starting with the insertion of the rupture disc into into the disc holder (the purple region above the rupture disc in figure 10), after first wetting the disc with isopropanol. While the disc dried, the macrocarrier assembly (the dark purple region in figure 10) was put together: the stopping screen was placed onto its shelf before the loaded macrocarrier holders were inverted and placed into the assembly above it. Once assembled, a lid (the light blue region, above the macrocarrier, in figure 10) was screwed into the assembly.

With both units assembled, the burst disc holder was screwed into the gas tube of the gun (the orange region in figure 10) using a torque wrench. Once this had been done, the

macrocarrier assembly was placed in its shelf, with the breech end of the assembly being directly below the burst disc assembly. Thereafter, the target could be loaded onto a tray (which includes a depression for placing 90mm petri dishes onto it) and the tray loaded into the gun below the macrocarrier assembly (labelled as the microcarrier launch assembly in figure 10). The distance from the assembly is controlled by placing the tray on a shelf, with shelves spaced at increments along the inside of the device.

After loading, the device was sealed and a vacuum drawn to the desired pressure. Once under vacuum, the device was armed and helium pumped from the regulator into the gas tube. The device fires once the burst disc reaches its pressure limit.
For all experiments, bombardments were done under vacuum (24 inches Hg) at a distance of 9cm from the muzzle of the device.

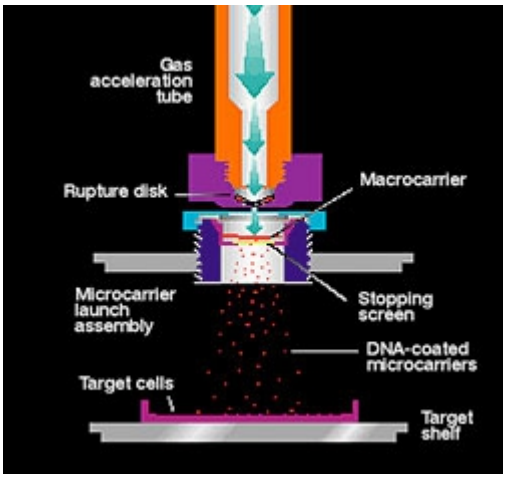

Figure 10. Schematic of biolistic bombardment process. Retrieved 2 March, 2014, from Bio-Rad Life Science Research: http://www.bio-rad.com/ja-jp/product/pds-1000-he-hepta-systems

13. Sample Staining and Analysis

Post-bombardment samples were wrapped in plastic and stored in the dark, at room temperature for 24 hours to allow for transient expression. After this period, sample staining was done using the laboratory standard 5-Bromo-4-chloro-1*H*-indol-3-yl β-D-glucopyranosiduronic acid (X-Gluc) histochemical stain solution protocol (adapted from Jefferson et al, 1987): 100mM phosphate buffer (pH 7); 10mM EDTA; 0.1% Triton X-100; 0.5mM K-ferricyanide; 0.5mM K-ferrocyanide; 0.521mg/ml X-Gluc (Thermo Fisher Scientific , Lithuania), dissolved in 200µl DMSO immediately prior to staining.

Samples were stained by immersion (with a 5 minute vacuum step) and were placed on a shaker for the duration of the staining step. Staining was carried out in dark, at 37°C, for 48-72 hours. Thereafter, samples were transferred to 70% ethanol and kept at 4°C until needed. In the final validation experiment a 55°C, 10 minute quenching step was used immediately prior to staining to suppress endogenous GUS activity (Hodal et al, 1992; Muhitch, 1998).

Microscopy and image analysis

Counting of foci (also referred to as 'spots') was done under a stereo dissecting microscope (Olympus SZX 10; 3x selection magnification), with foci being manually logged and scored. Once scored, samples were hand-sectioned and mounted for microscopic analysis using a stereo-microscope (Zeiss Axioskop; 10, 20 or 40X objective magnification). The subsequent images were not digitally altered aside from the addition of scale bars.

Hand cryo-sectioning technique

To achieve sections of suitable thickness for the purposes of the experiments, an improved form of hand-sectioning (hand cryo-sectioning) was developed. In this protocol, samples were fixed between pieces of carrot produced using a 1cm diameter coring apparatus. The cores were then split at the ends using a razor blade, the sample placed inside and the tip bound up using a small plastic cabletie. The bound samples were then wetted at the tip before being placed vertically in a container and stored for at least half an hour in a -70°C freezer.

When microscopic analysis was to be performed, the samples were removed from storage, their tips dipped in water and then hand-sectioned in the conventional way. Once the cable tie was reached, it was carefully levered off and the sample re-frozen before continuing. In this fashion, a number of very thin slices could be obtained for wet-mount microscopy. These slices, once mounted, were then analysed under stereo-microscope (same make, model and conditions as with hand sections).

14. Data analysis

Taguchi methodology

The standard Taguchi design-of-experiments and analysis approach was followed (Taguchi, 1986; Roy, 1990), with a four-factor/3-level design being used. Orthogonal arrays (L9 arrays) were generated from the chosen input factors, and used to design nine trials or sub-experiments. After the trial data was gathered, the optimisation proceeded according to standard protocols (Roy, 1990). Signal-to-noise ratio analysis was performed, with the biggest-is-best performance characteristic being chosen for optimisation. Main effect analysis was used to generate optima.

Statistical analysis

Prof Steffens (University of Pretoria Department of Statistics) assisted in performing statistical analysis of the data generated by the Taguchi optimisation experiment. To do so, he used the SPSS statistical software package to perform analysis. The data was then used to produce a generalised linear model, which was then used for optima prediction.

Other data analysis was performed using Open-office Calc (with appropriate macros for more advanced statistical analysis) and R with Rattle plugin. (Retrieved 16 April, 2014, from Togaware: http://rattle.togaware.com/).

Non-parametric and ranking methods were used for verification of statistically-meaningful differences between sample populations. The Kolmogorov-Smirnov test was used to check for distribution differences, with the Wilcoxon rank sum test (equivalent to the Wilcoxon-Mann-Whitney test) being used to assess differences in median between sample sets. The results were tested against a 95% confidence level (P-value <= 0.05 to reject null hypothesis). Cell size analysis was done using a standard Student's t-test.

Results

In all cases, the primary experimental output being analysed was the blue-stained focus (or 'spots') obtained when reacting beta glucuronidase-expressing cells with X-gluc stain solution (figure 11). These spots were used as a proxy for transformation efficiency as, in nearly all cases, each corresponded to a single transiently expressing cell.

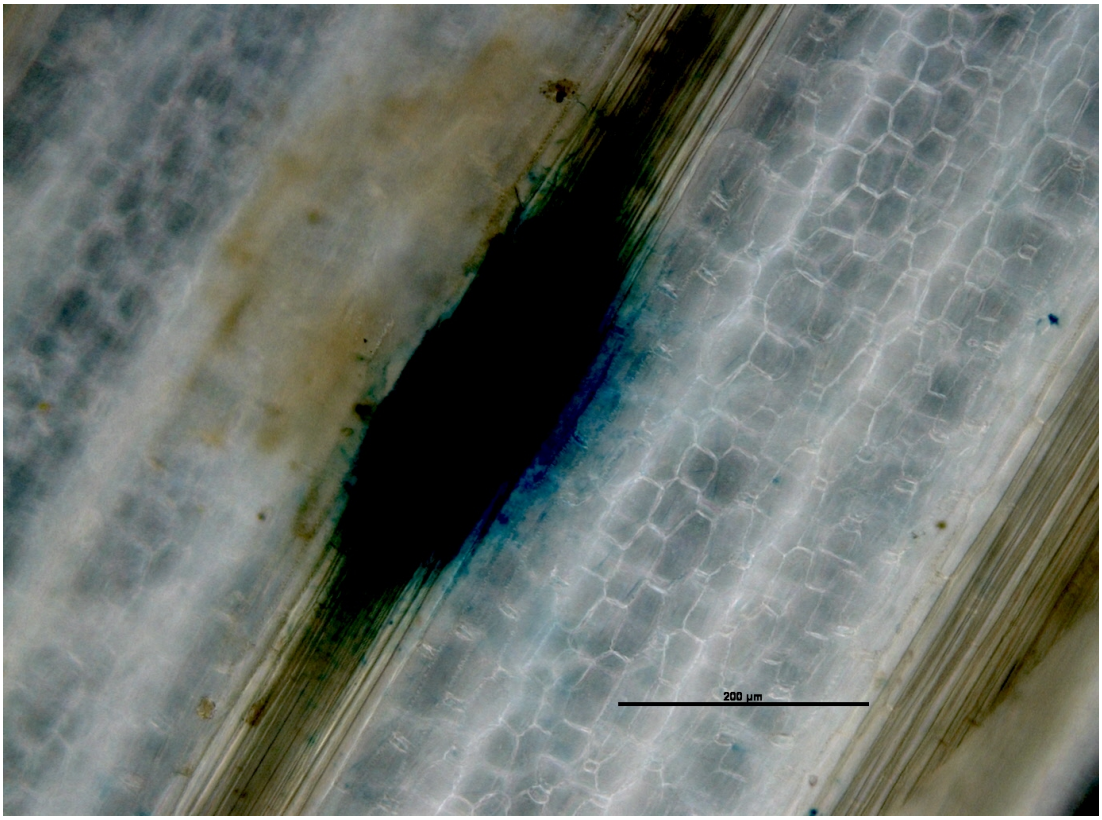

Figure 11. Histological staining of beta glucuronidase (GUS)-expressing cells after bombardment, seen on the adaxial surface of a media-grown maize leaf. This large focus was obtained during the baseline expression experiment.

During the course of the optimisation study, three major experiments were performed. The first was a baseline expression experiment, meant to provide a useful estimate of the existing laboratory bombardment protocols and to test procedures for subsequent experiments. The second experiment was intended to optimise the existing protocols using Taguchi design-of-experiments and analysis (the so-called Taguchi method). This consisted of two major parts: a series of trials using different input conditions (determined as part of the experimental design); followed by quantitative analysis, optimisation and optima projection of the data generated by these trials.
Finally, an experiment was performed to verify the optimised protocol by comparing it

directly to the baseline conditions. This also included a sub-experiment testing the effect of another factor (distance from leaf base, measured from the ligule) identified in the literature (Kirienko et al, 2012).

15. Baseline expression experiment

Baseline expression was tested using standard laboratory conditions for maize bombardments (Frame et al, 2000). Plasmid visual marker gene construct pAHC25 was used as a vector, at a concentration of 3ug/µl ($4.76x10^{-13}$ umol/µl). DNA loading was 5ug ($2.38x10^{-6}$ umol) per bombardment. M17 tungsten microcarriers (approximately 1.1um) were used, with 0.2ug being used per bombardment. Burst disc pressures of 900PSI were used. Samples were taken according to Kirienko et al (2012), with the 'inner' non-emergent leaves being used. The maize samples used in this experiment were taken from media-grown B73 plantlets.

The expression seen in this experiment was low overall, with a large percentage of samples showing no expression at all (figure 12).

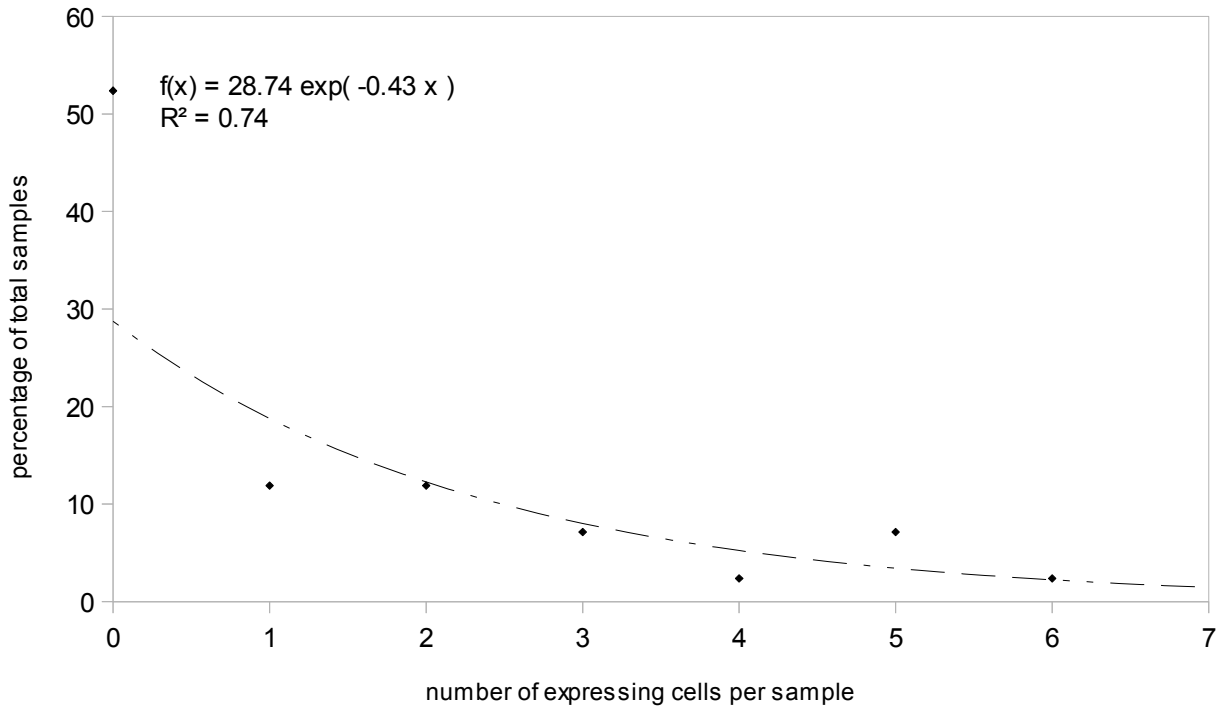

Figure 12. Frequency distribution of baseline expression experiment. Outliers above 7 spots per sample (approx 5% of total samples) have been excluded for clarity

16. Taguchi optimisation experiment

Taguchi optimisation, using a orthogonal array-based design of experiments (Taguchi, 1986; Roy, 1990), was carried out for four input factors: DNA loading, particle loading, burst disc pressure and placement within the non-emergent leaf whorl. Each factor was assessed using three intensity levels (generally a low, medium and high concentration/value of the given factor), giving a total of 81 possible combinations of factors and levels to test.

The Taguchi design-of-experiment approach makes use of orthogonal array-based trial designs, of which a number have been published (Roy, 1990). By cross-referencing the number of factors and number of levels for each factor, a suitable array with suggested inputs can easily be found using an array selector table. From here, the recommended array (L9) projected that nine trials would be needed; with the intensity of each factor tested three times for each level (table 4).

Table 4. Experimental conditions for Taguchi optimisation experiment.

Trial number	Burst disc pressure (PSI)	Particle load (mg) per bombardment	DNA load (ug) per bombardment	Sample position within non-emergent leaf whorl
1	650	0.2	2.5	Outer non-emergent
2	650	0.4	5	Inner non-emergent
3	650	0.75	7.5	Central whorl
4	900	0.2	5	Central whorl
5	900	0.4	7.5	Outer non-emergent
6	900	0.75	2.5	Inner non-emergent
7	1350	0.2	7.5	Inner non-emergent
8	1350	0.4	2.5	Central whorl
9	1350	0.75	5	Outer non-emergent

The optimisation experiment, once performed, resulted in the largest overall sample pool; with highly variable responses to input parameters seen amongst the various sub-trials (figure 13). Once the nine trials had been completed and the resulting samples assessed, an in-depth analysis of the trial data was undertaken.

Firstly, standard statisical approaches were used to examine sample subsets sharing input characteristics. Then Taguchi analysis was performed to determine optimum conditions and project the resultant expression expected from these conditions. This was then compared against the output of the generalised linear model developed by Prof. Steffens of the University of Pretoria department of Statistics.

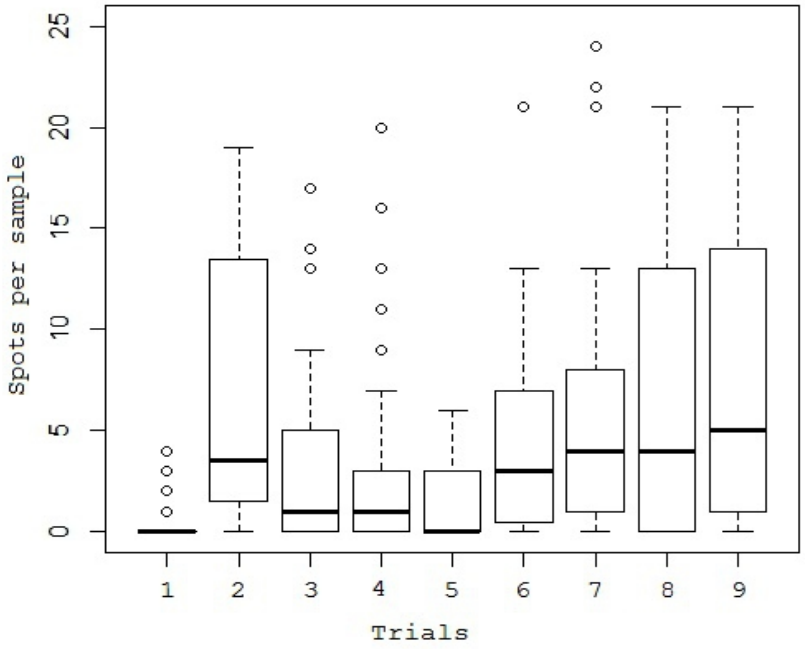

Figure 13. Box plot of trial results for Taguchi optimisation experiment. Trial numbers correlate to those in table 4. Outliers above 25 (approx. 5% of total samples) have been excluded for clarity.

17. Analysis of Optimisation Experiment Data: Comparison Within Sample Subsets

In order to assess the effect of the tested factor levels, samples were pooled according to input factor and the results analysed statistically. Due to the non-normal nature of the data, a non-parametric test (the Wilcoxon rank-sum test) was used to determine if the medians of the sample subsets were significantly different. For this purpose the statistical program R was used, which outputs both the W-statistic (which is simply required to produce the ranking probability distribution) and the p-value for each comparison. In the case of the summary tables for each sample subset (tables 5, 7, 9 and 11), the chosen optimal conditions used for the validation experiments (outlined on page 50) have been highlighted for reference.

17.1 The effect of burst disc pressure on expression

Sample sub-sets were generated by grouping trial results according to burst disc pressure, with the results being recorded in table 5. Wilcoxon rank-sum testing (table 6) was then performed on the samples to determine if sample medians differed between factor levels. The results of this testing demonstrate a significant difference between the high burst disc pressure level (1350PSI) and the rest of the subset, with the 1350 PSI sample subset producing a higher median level of expression. This can be seen graphically in figure 14.

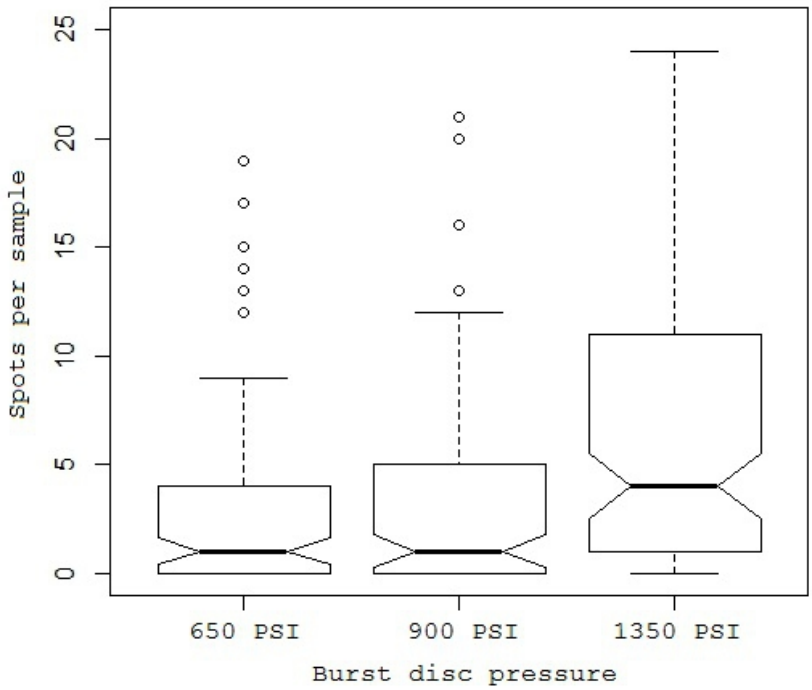

Figure 14. Notched box plot of pressure versus transformation efficiency. Outliers above 25 spots per sample (approx. 5% of total samples) have been excluded for clarity

Table 5. Samples separated into subgroups according to burst disc pressure. Highlighted samples represent the chosen optimal values tested in the validation experiment.

Samples	Median spot count	Mean spot count	Maximum spot count	Standard deviation	Summed spot count
650PSI	1	3.96	51	7.96	420
900PSI	1	3.8	45	6.57	426
1350PSI	4	10.55	111	17.04	1129

Table 6. Comparison of burst disc pressure sample subset medians (Wilcoxon rank-sum)

Samples	W-statistic	p-value	Is null hypothesis rejected? ($p < 0.05$)
650PSI : 900PSI	5464.5	0.29	NO
650PSI : 1350PSI	3601	2.60×10^{-6}	YES
900PSI : 1350PSI	4105.5	4.35×10^{-5}	YES

17.2 The effect of tungsten microparticle loading on expression

Sample sub-sets were generated by grouping trial results according to microparticle loading, with the results being recorded in table 7. Wilcoxon rank-sum testing was then performed on the samples to determine if sample medians differed between factor levels (table 8).

These demonstrated no statistical difference between the two higher factor levels (0.4 and 0.8mg of tungsten particle per bombardment), but showed both to be statistically different from the lowest factor level tested (0.2mg). This, as demonstrated by figure 15, suggests a broad optima above a critical level of loading.

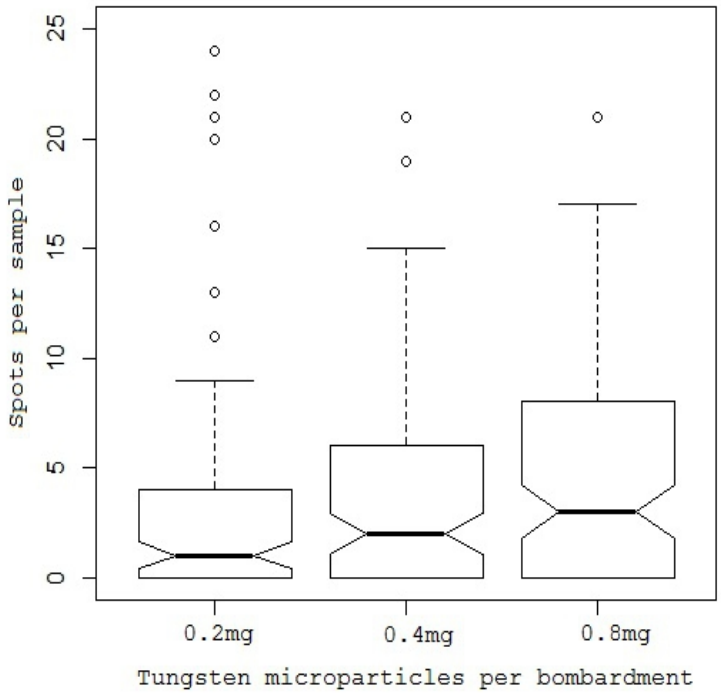

Figure 15. Notched box plot of particle load versus transformation efficiency. Outliers above 25 spots per sample (approx. 5% of total samples) have been excluded for clarity.

Table 7. Samples separated into subgroups according to tungsten loading . Highlighted samples represent the chosen optimal values tested in the validation experiment.

Samples	Median spot count	Mean spot count	Maximum spot count	Standard deviation	Summed spot count
0.2mg per bombardment	1	4.24	45	8.07	467
0.4mg per bombardment	2	7.5	111	15.13	787
0.75mg per bombardment	3	6.56	65	11.3	721

Table 8. Comparison of tungsten loading sample subset medians (Wilcoxon rank-sum)

Samples	W-statistic	p-value	Is null hypothesis rejected? ($p < 0.05$)
0.2mg : 0.4mg	4819.5	0.03	YES
0.2mg : 0.75mg	4740.5	0.04	YES
0.4mg : 0.75mg	5468.5	0.5	NO

17.3 The effect of DNA loading on expression

Sample sub-sets were generated by grouping trial results according to DNA loading, with the results being recorded in table 9. Wilcoxon rank-sum testing was then performed on the samples to determine if sample medians differed between factor levels (table 10). This analysis indicated a mid-range optima (5ug pAHC25 DNA per bombardment). This is illustrated by figure 16.

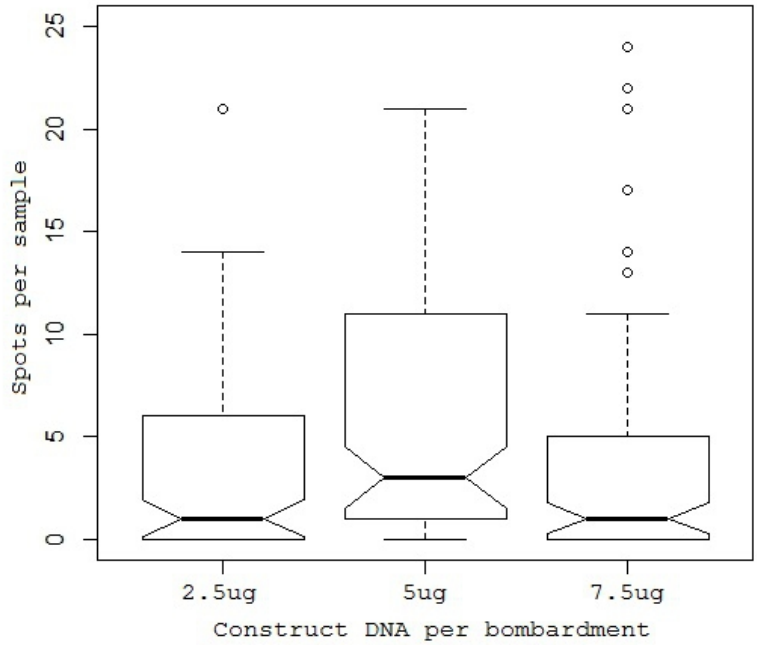

Figure 16. Notched box plot of DNA loading versus transformation efficiency. Outliers above 25 spots per sample (approx. 5% of total samples) have been excluded for clarity

Table 9. Samples separated into subgroups according to DNA loading. Highlighted samples represent the chosen optimal values tested in the validation experiment.

Samples	Median spot count	Mean spot count	Maximum spot count	Standard deviation	Summed spot count
2.5ug per bombardment	1	5.91	111	13.95	639
5ug per bombardment	3	8.24	65	13.19	906
7.5ug per bombardment	1	4.02	35	6.63	430

Table 10. Comparison of DNA loading sample subset medians (Wilcoxon rank-sum)

Samples	W-statistic	p-value	Is null hypothesis rejected? ($p < 0.05$)
2.5ug : 5ug	4623	$3.9x^{10-3}$	YES
2.5ug : 7.5ug	5704.5	0.87	NO
5ug : 7.5ug	7117.5	$6.6x^{10-3}$	YES

17.4 The effect of sample position within leaf whorl on transgene expression

Sample sub-sets were generated by grouping trial results according to sample location within the non-emergent leaf whorl, with the results being recorded in table 11. Wilcoxon rank-sum testing was then performed on the samples to determine if sample medians differed between factor levels (table 12). The results show that, despite a higher median (figure 17), the central whorl and inner non-emergent leaf samples could not be distinguished at high statistical significance. This suggests that, much as with tungsten loading, there is simply a lower bound (ie: a certain depth into the non-emergent leaf whorl at which samples should be taken) rather than a defined optimal point for this factor.

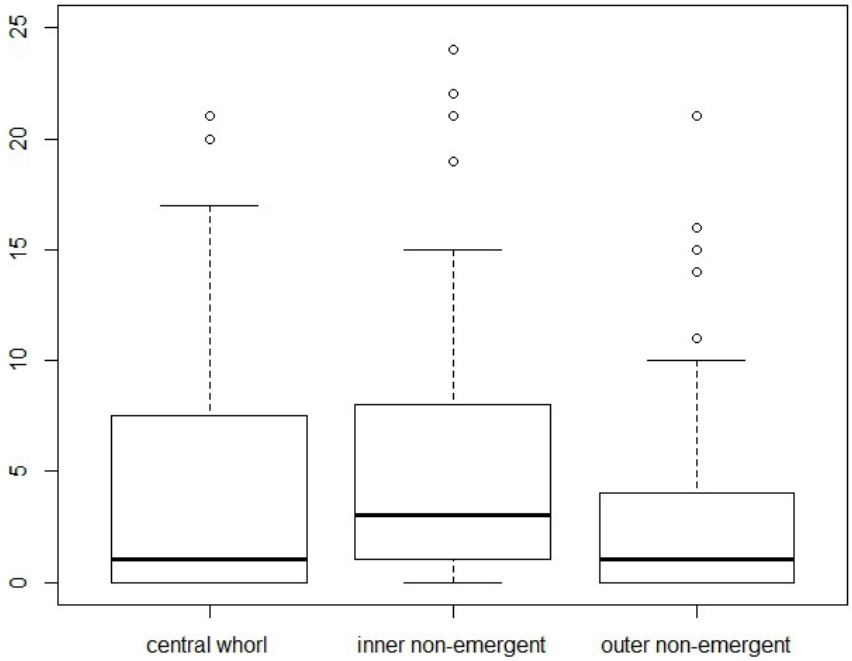

Figure 17. Box plot of sample placement within non-emergent leaf whorl versus transformation efficiency. Outliers above 25 spots per sample (approx. 5% of total samples) have been excluded.

Table 11. Samples separated into subgroups according to location within the non-emergent leaf whorl. Highlighted samples represent the chosen optimal values tested in the validation experiment.

Samples	Median spot count	Mean spot count	Maximum spot count	Standard deviation	Summed spot count
Central whorl leaves	1	6.89	111	14.72	716
Inner non-emergent leaves	3	6.83	51	9.2	765
Outer non-emergent leaves	1	4.53	65	11.1	494

Table 12. Comparison of leaf whorl sample subset medians (Wilcoxon rank-sum)

Samples	W-statistic	p-value	Is null hypothesis rejected? ($p < 0.05$)
Outer non-emergent : inner non-emergent	4089	1.45×10^{-5}	YES
Outer non-emergent : central whorl	4968.5	0.1	NO
Inner non-emergent : central whorl	6951.5	0.01	YES

18. Analysis of Optimisation Experiment Data: Taguchi Analysis

The application of the Taguchi method of optimisation rests on the testing and analysis of multiple factors in a given system. This analysis, when applied, consists of three procedures. The first, signal-to-noise ratio analysis, gives an indication of the relative response that the tested variable has to changes in the chosen input factors. This can strengthen or weaken subsequent conclusions drawn from further analysis.

The second procedure, the main effect plot, simply plots the means of each factor level graphically to assist in the selection of optimal levels for each factor. Finally, the scores under optimum conditions can be projected by calculating the marginal means of each level (the mean of each factor minus the global mean) and adding the scores together with the global mean to obtain a projected score.

18.1 Signal-to-noise ratio analysis

S/N ratio calculations

As the maximum performance characteristic was being sought, the signal-to-noise ratio equation becomes (Roy, 1990):

$$SN_i = -10 \log \left[\frac{1}{N_i} \sum_{u=1}^{N_i} \frac{1}{y_u^2} \right]$$

This means that the signal-to-noise ratio for a given dataset (SN_i) is equal to the negative log of the inverse sum of squares of its components ($1/y^2_u$), multiplied by the inverse of the number of samples ($1/N_i$).

Once applied, this resulted in a S/N ratio for each experiment (table 13). These ratios were positive, but low. For comparison, the lowest practicable signal-to-noise ratio score (as 1/0 is infinite and the spots are counted as whole numbers rather than fractions) will be zero in this case, with a score of 20 being obtained if all samples in the dataset show 10 spots.

Table 13. Signal-to-noise ratio for each trial within the Taguchi optimisation experiment.

Trial	S/N ratio	Average spot count
1	8.74	0.42
2	8.48	8.36
3	7.61	3.06
4	7.68	4.86
5	8.25	1.5
6	8.54	4.92
7	9.05	7.35
8	7.49	13.09
9	8.67	11.49
Global mean		6.08

S/N ranking for all factors

Once S/N ratios had been calculated for all trials, the results were pooled by factor and averaged to produce a mean ratio for ranking studies (table 14). The lowest mean ratio in for each factor was then subtracted from the highest to produce a difference measurement score. Ranking was done based on difference, with the highest score being assumed to affect the mean in the most consistent, linear fashion. Scores indicated that microparticle loading was the top-ranking factor.

As ranking is dependent on the difference between scores, a fractional score indicates a very low response to signal. Using a hypothetical example, the difference between a sample group consisting entirely of single-spot samples (resulting in an score of zero) and double-spot samples (resulting in a score of ~6) is 6. Similarly, the difference between sample groups with 2 and 3 spots (resulting in a score of ~ 9.5) is still around 3.5. Even small increases in transformation efficiency would thus register as larger numbers than is

seen in the experiment.

The results of table 14, therefore, indicate an extremely weak response to signal for all of the factors tested. This indicates that there will always be a lot of uncertainty when separating or comparing response to factors in this system.

Table 14. S/N ranks for all factor subgroups, with the effect of factor intensity on ranking score being shown

	S/N rank for			
Factor intensity	**Burst disc pressure**	**Microparticle loading**	**DNA loading**	**Sample position within non-emergent leaf whorl**
Low (650PSI, 0.2mg, 2.5ug; outer non-emergent)	8.28	8.49	8.25	8.55
Medium (900PSI, 0.4mg, 5ug; inner non-emergent)	8.15	8.07	8.27	8.69
High (1350PSI, 0.75mg, 7.5ug; central whorl)	8.4	8.27	8.3	7.59
Difference between highest and lowest S/N per factor	0.24	0.42	0.05	0.14
Rank	**2**	**1**	**4**	**3**

18.2 Main effect plot

Main effect plots were generated by pooling all samples sharing a single factor and creating factor means from the pooled data. These means were then plotted for each factor level (figure 18). The plot indicated that the optimum levels for each factor were: a DNA loading of 5ug ($2.38x10^{-6}$ umol), microparticle (tungsten) loading of 0.4mg, burst disc pressure of 1350PSI and selection of samples from the deepest (central) part of the non-emergent leaf whorl.

The plot also indicated that, in the case of microparticle loading and sample selection, the differences between the two best-performing factors were minimal.

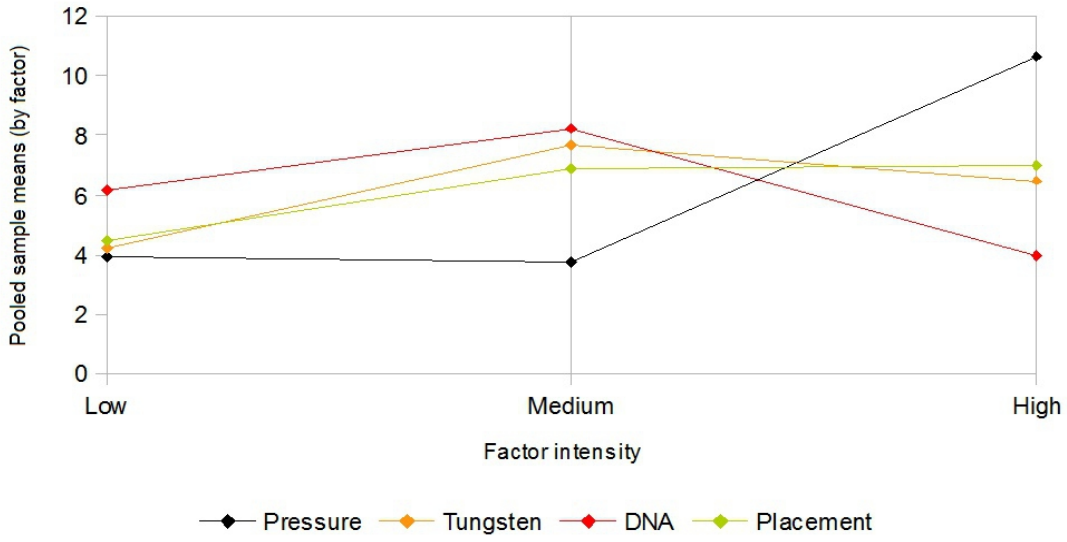

Figure 18. Main effect plot of all factors and levels. The given intensities for each factor level correspond to those described in table 14.

18.3 Optima projection

Projections for new factor combinations were made using pooled sample means, with mean contribution score being determined by subtraction of the global mean of 6.08 spots per sample (table 15). The most positive contributing factors are in bold.

Table 15. Contribution table for optima projections.

Factor intensity	Burst disc pressure	Microparticle loading	DNA loading	Sample position within non-emergent leaf whorl
Low (650PSI, 0.2mg, 2.5ug; outer non-emergent)	-2.13	-1.87	0.07	-1.61
Medium (900PSI, 0.4mg, 5ug; inner non-emergent)	-2.31	**1.57**	**2.16**	0.8
High (1350PSI, 0.75mg, 7.5ug; central whorl)	**4.66**	0.41	-2.11	**0.93**

Using this approach, the projected baseline and optimal means can be determined:
Baseline conditions (by using equivalent values to the baseline experiment from table 15) = 6.08 (the global mean; see table 13) - 2.31 - 1.87 + 2.16 + 0.8 = **4.86** spots per sample

Projected optimal conditions (by taking highest contribution scores from table 15) = 6.08 + 4.66 + 1.57 + 2.16 + 0.93 = **15.40** spots per sample

19. Analysis of Optimisation Experiment Data: Generalised Linear modelling

Having performed Taguchi optimisation, the next step is to validate the statistical accuracy of the projected optima using conventional tools and approaches such as ANOVA (Taguchi, 1986). At this point, it was determined that the highly variable nature of the data produced by the experiments, combined with a non-normal distribution and large outliers (discussed further in the subheading 'summary of data quality' on page 54) meant that the recommended techniques could not be followed further.

Model development

Due to the statistically problematic nature of the data, the results of the Taguchi optimisation experiment were taken to Prof. Steffens at the University of Pretoria department of Statistics, who used the SPSS statistical software package to develop a Generalised Linear Model (GLM). The purpose of the model was initially to assess the chosen optimal conditions. However, the model was also capable of producing projections of factor combinations, in effect allowing all 81 possible factor combinations to be simulated. Initial model components were a Poisson distribution function and Log link function, with the number of expressing spots per sample being used as a dependant variable. Once tree building had been carried out the model was tested for goodness-of-fit and used to generate marginal means estimates (table 16)

Table 16. Estimated marginal means for all factors and levels, as indicated by GLM. Optimal conditions are bolded.

Factor		Mean	Standard error
Burst disc pressure			
	650 PSI	2.2	0.21
	900 PSI	3.3	0.19
	1350 PSI	**9.46**	**0.3**
Microparticle loading			
	0.2mg	2.46	0.23
	0.4mg	5.01	0.26
	0.75mg	**5.57**	**0.24**
DNA loading			
	2.5ug	2.74	0.25
	5ug	**7.76**	**0.27**
	7.5ug	3.23	0.19
Location within non-emergent leaf whorl			
	Central	5.3	0.24
	Inner	**6.71**	**0.19**
	Outer	1.93	0.25

Response Prediction

The model, once developed, was used to make predictions on the sample means of all 81 possible combinations of factors and intensities. Using these predictions, a calculated optimum was determined: a DNA loading of 5ug, microparticle (tungsten) loading of 0.75mg, burst disc pressure of 1350PSI and selection of samples from the inner leaves of the non-emergent leaf whorl. This was also used to to determine the projected mean baseline and optimal expression levels, indicating that baseline conditions would result in an average of 6 spots per sample while the projected optimal conditions would produce 40 spots. This was a more optimistic projection than that provided by the Taguchi analysis: the Taguchi optimum conditions, for instance, were projected at 28 spots per sample (by looking at the predicted spot count for the combination of factors selected using Taguchi optimisation). Conversely, the Taguchi projection for the GLM-derived optima, while lower, was quite similar to the Taguchi-derived optimum:14.1 vs. 15.4 spots per sample (using the same approach as the Taguchi projections and the information from table 15).

Having generated and examined two sets of optima using two different approaches (Taguchi's main effect plot and optima projection versus the projections outputted by the GLM), it was decided to use the GLM-developed optima (discussed in the subsection

'development and testing of optimised conditions' on page 61).

20. Analysis of Optimisation Experiment Data: Comparison of projected optimal conditions

Figure 19 summarises the different optima chosen by application of the Taguchi method, as well as the optima generated by the Generalised Linear Model constructed from the same dataset. In general, the choice of optimal factor level (as discussed below) is directly correlated with the statistical strength of the different expression levels associated with each factor.

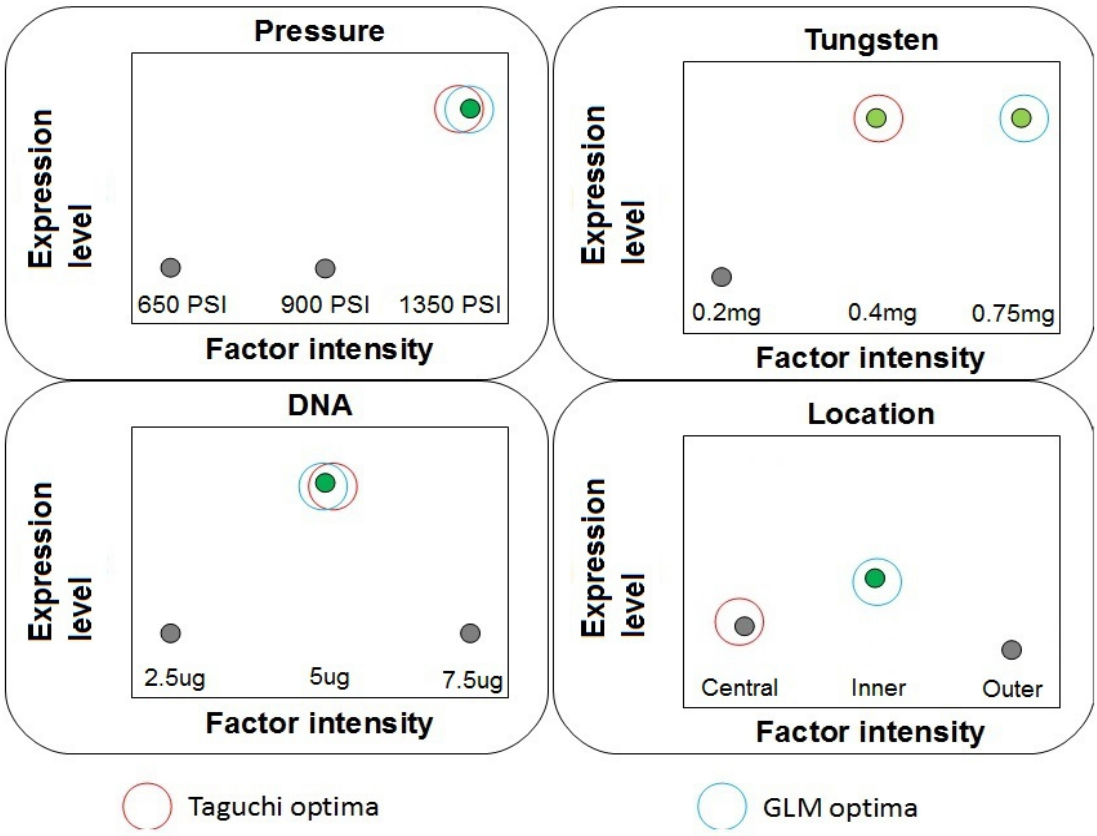

Figure 19. A summary of the Generalised Linear Model (GLM) and Taguchi results, with reference to the statistical significance of each factor level. Note the differing optima presented for microparticle loading (tungsten) level – where the superior factor levels are statistically indistinguishable – and for location within the leaf whorl (location) where they are both distinguishable (albeit at low statistical resolution) and indicate different optima.

21. Verification of Optimal Conditions

An experiment to validate the chosen optimal conditions was performed, divided into a number of trials with baseline and optimised conditions being tested in four trials each (figure 20, table 17). Within this experiment a new factor (sample distance along the leaf axis from the ligule) was also tested, with the two levels for that factor being tested four times. Experiments 1/5, 2/6, 3/7 and 4/8 were thus direct replicates.

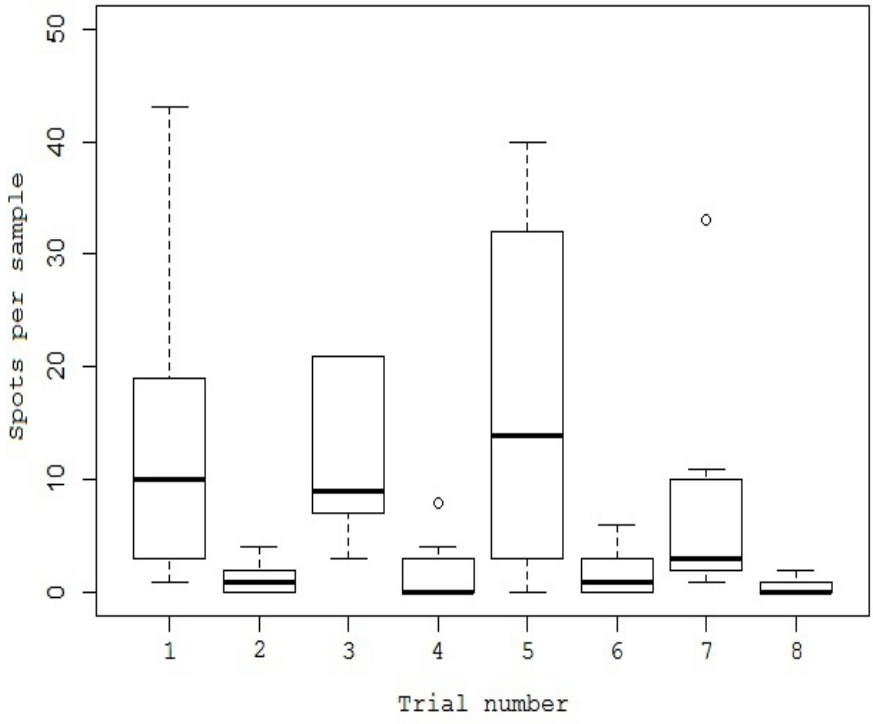

Figure 20. Box plot of verification experiment results. Trial numbers are as in table 17. Outliers above 50 spots per sample (approx. 3% of total samples) have been excluded for clarity.

Table 17. Experimental conditions for trials during optima validation experiment

Trial number	Burst disc pressure (PSI)	Particle load (mg) per bombardment	DNA load (ug) per bombardment	Sample position within non-emergent leaf whorl	Distance along leaf axis from ligule
1	1350	0.75	5	Inner non-emergent	0 - 3cm
2	1350	0.75	5	Inner non-emergent	3 - 6cm
3	900	0.2	5	Inner non-emergent	0 - 3cm
4	900	0.2	5	Inner non-emergent	3 - 6cm
5	1350	0.75	5	Inner non-emergent	0 - 3cm
6	1350	0.75	5	Inner non-emergent	3 - 6cm
7	900	0.2	5	Inner non-emergent	0 - 3cm
8	900	0.2	5	Inner non-emergent	3 - 6cm

Once the trials were performed and the resulting expression levels quantified by microscopy, the data was pooled, analysed and compared within trial groups (figures 21 and 22). From this it can be shown that the sample distributions are significantly different across multiple experiments. The strongest difference is between the 0-3cm and 3-6cm ligule-distance subsets from the validation experiment (figure 21).

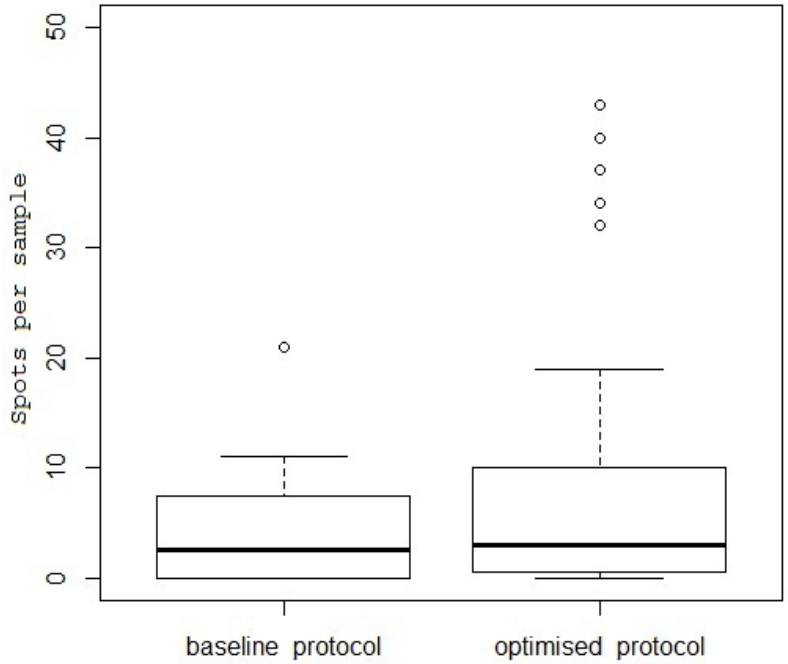

Figure 21. Box plot of the baseline vs. optimised expression sample subsets. Outliers above 50 spots per sample (approx. 3% of total samples) have been excluded for clarity.

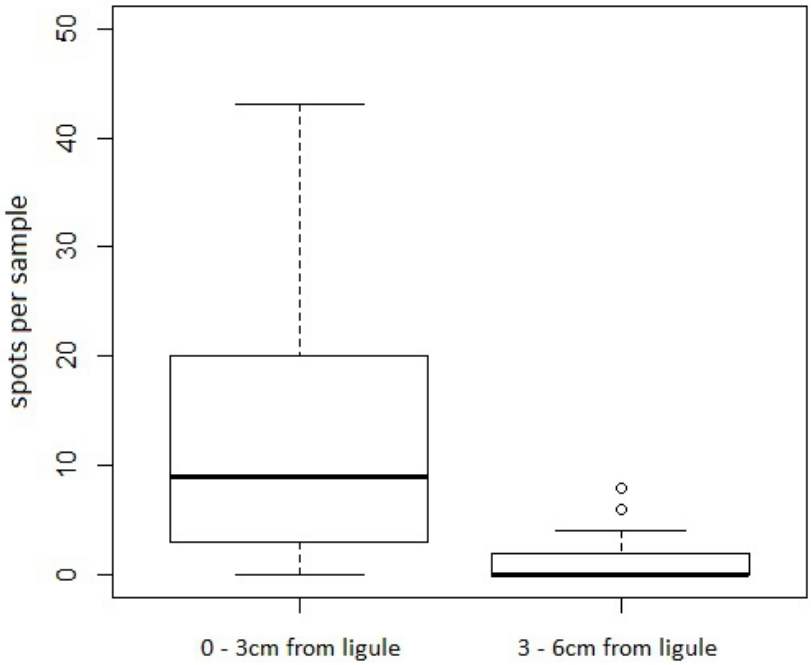

Figure 22. Box plot comparing expression efficiencies for sample subsets along the leaf axis from the ligule. Outliers above 50 spots per sample (approx. 3% of total samples) have been excluded for clarity.

Two-sample Kolmogorov-Smirnov tests were done to check the distributions of all major sample groups against each other (table 18). This was necessary as the data was not normally-distributed, but also gave an indication of the similarities across datasets.

Table 18. Distribution comparisons between various experiments and sample subsets using the Kolmogorov-Smirnov test

Samples	D-statistic	p-value	Is null hypothesis rejected? ($p < 0.05$)
Baseline experiment : Taguchi optimisation experiment	0.25	0.02	YES
Baseline experiment : Validation experiment	0.28	0.04	YES
Baseline experiment : Validation experiment (baseline conditions)	0.26	0.14	NO
Taguchi optimisation experiment : Validation experiment	0.08	0.85	NO
Validation (baseline conditions) : Validation (optimised conditions)	0.11	0.98	NO
Validation (0-3cm from ligule) : Validation (3-6cm from ligule)	0.64	8.31×10^{-7}	YES

Figure 23 illustrates the change in frequency distribution (as confirmed in table 18) between the 0-3 and 3-6cm ligule distance groups. One of the most striking aspects of these two sample subsets is the small number of non-expressing samples seen in the 0-3cm subgroup. This goes against all previous data, which generally show that around half of the samples tested will not develop any spots.

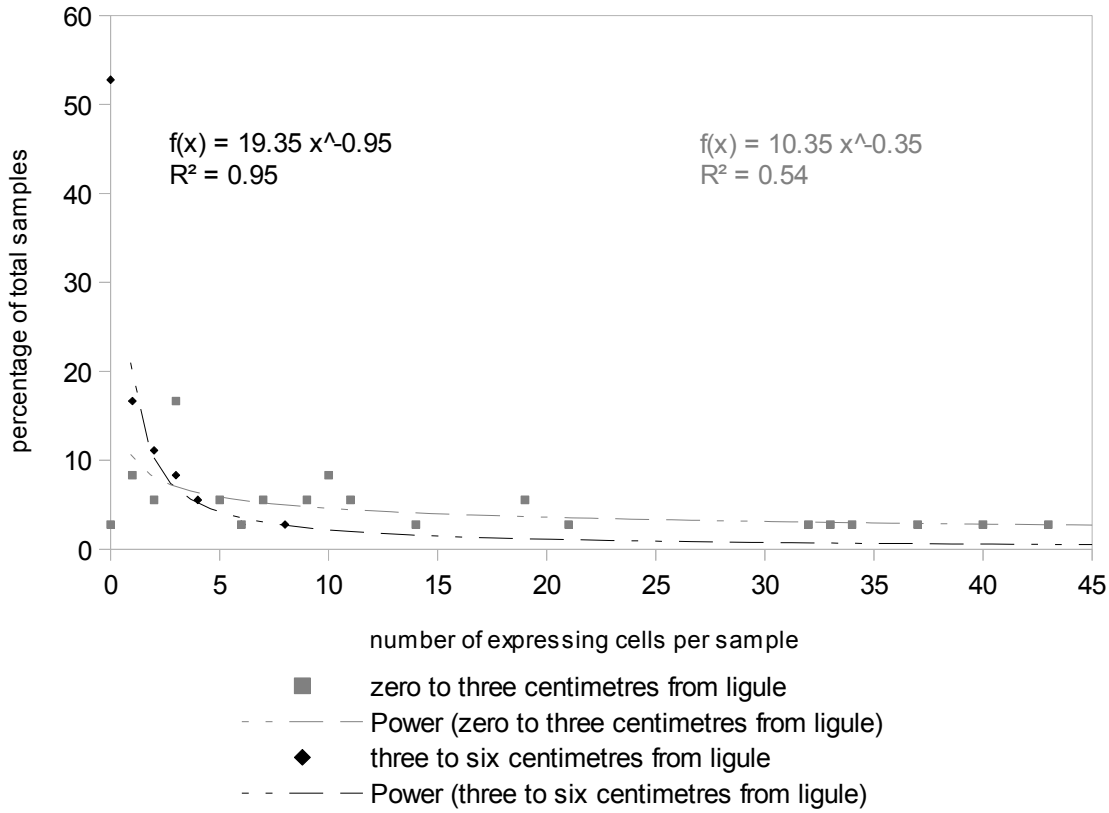

Figure 23. Frequency distributions for the ligule-distance sample subsets of the validation experiment. Data is for the bottom 95% of samples (2 samples excluded)

Two-sample Wilcoxon ranked-sum tests were then done on selected sample sets, to determine if they showed statistically different medians (table 19).

Table 19. Median comparison between various experiments and sample subsets using the Wilcoxon ranked-sum test

Samples	W-statistic	p-value	Is null hypothesis rejected? ($p < 0.05$)
Baseline experiment : Validation experiment	980	1.32×10^{-3}	YES
Baseline experiment : Validation experiment (baseline conditions)	516	0.01	YES
Taguchi optimisation experiment : Validation experiment	10691	0.24	NO
Validation (baseline conditions) : Validation (optimised conditions)	601.5	0.6	NO
Validation (0-3cm from ligule) : Validation (3-6cm from ligule)	1169	2.86×10^{-9}	YES

22. Summary of data quality

Numbers of beta glucuronidase-expressing cells ('spots') per sample were assessed by direct observation under low magnification. Overall, the data showed high variation and a strong skewing of samples towards zero/low expression (as seen in table 20). This made standard statistical approaches (t-tests, ANOVA) less reliable, so non-parametric methods (Kolmogorov-Smirnov test and Wilcoxon rank-sum test) were used to evaluate data instead.

Table 20. Summary of results

Samples	Maximum spot count	Mean spot count	Standard deviation from mean	Median spot count	Number of samples
Baseline experiment	12	1.4	2.5	0	42
Taguchi optimisation experiment (all samples)	65	5.9	10.6	3	324 (36 per trial)
Validation experiment (all samples)	156	10.9	24.3	3	72
Validation Experiment (baseline conditions)	156	13.8	33.5	2.5	36
Validation Experiment (optimised conditions)	43	10.5	14.7	3	36
Validation Experiment (0-3cm from ligule)	156	20.8	33.2	9	36
Validation Experiment (3-6cm from ligule)	8	1.5	2.2	0	36

23. Microscopy

23.1 Spot density of samples along the leaf axis

Samples were directly mounted for microscopic analysis of histological staining under dissecting microscope. By observation, it was found that samples taken from close to the leaf ligule tended to show more compact spot morphologies than samples further along the leaf axis (figure 24). The 'spots' observed in the figure are a result of histochemical staining of the X-gluc substrate caused by beta-glucuronidase (GUS) expression. The expression, in turn, is the result of transient transformation due to bombardment with particles carrying the pAHC25 plasmid, which contains a GUS reporter gene construct.

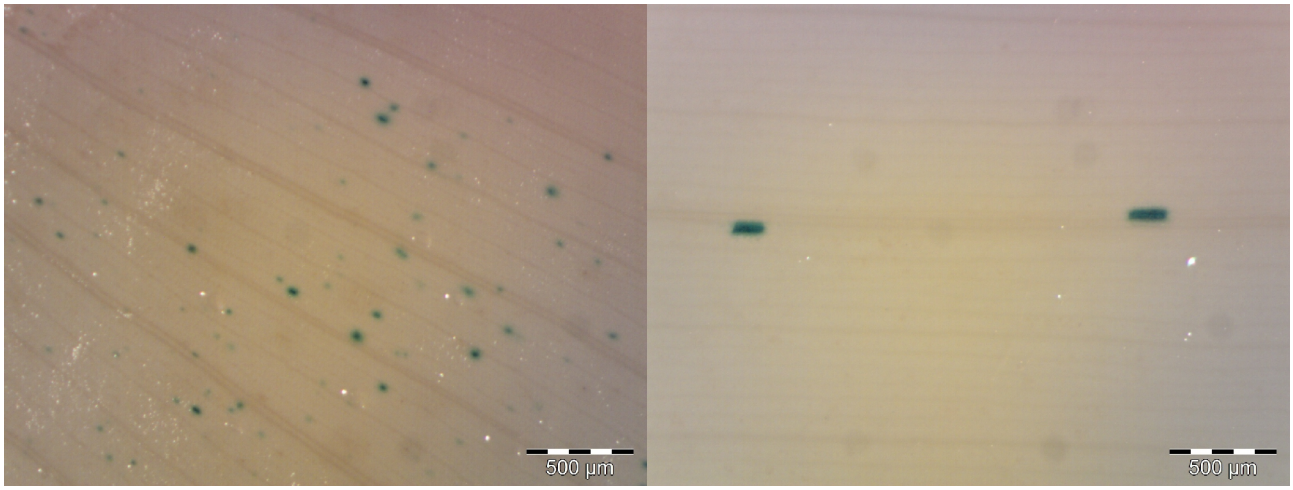

Figure 24. Differing spot densities and morphologies seen in sample subgroups 0-3cm (left image) and 3-6cm (right image) from leaf ligule.

23.2 Depth of penetration of microcarriers

During microscopic examination of dissected samples, it was noted that no expression below a depth 100um was observed (figure 25).

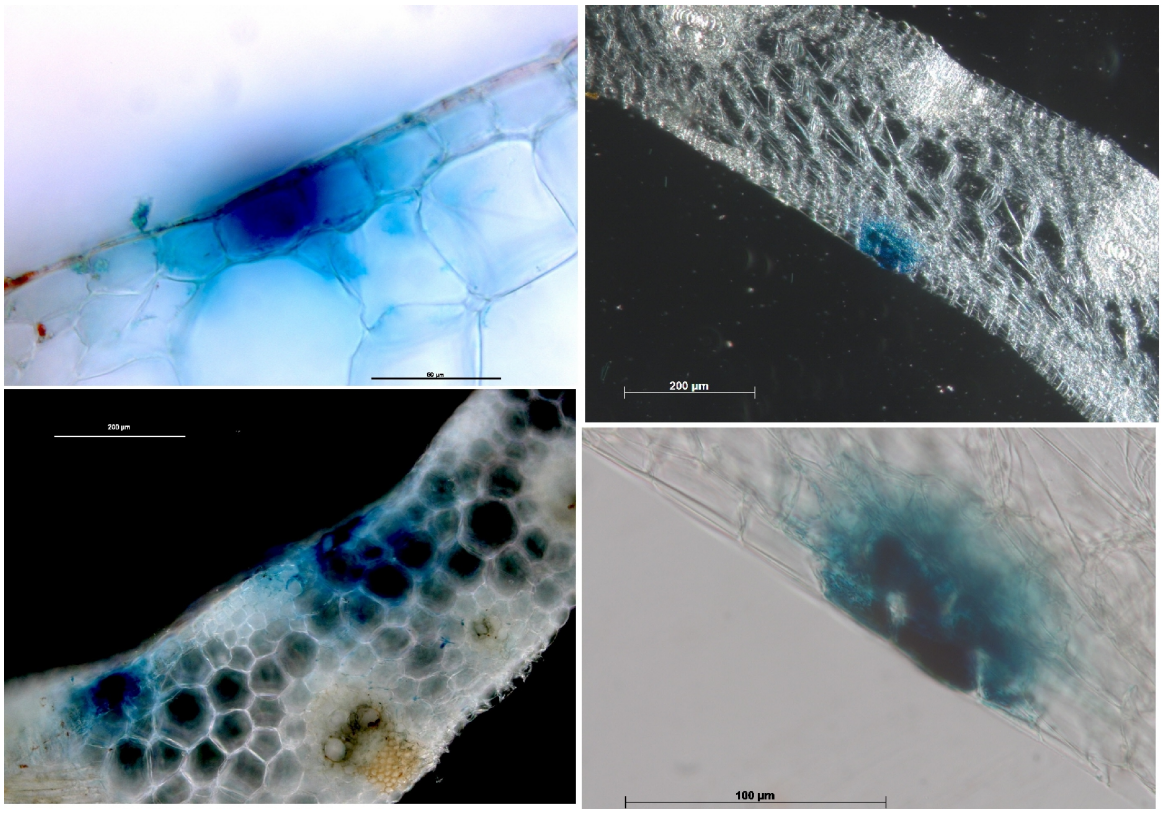

Figure 25. Composite picture showing typical staining patterns for bombarded samples. Samples are all transverse sections of histochemically-stained tissue, produced using standard hand-sectioning approaches.

Cell size analysis

Hand cryo-sectioning of the samples was done to determine the relative cell sizes of the samples in the 0-3 and 3-6cm ligule distance groups. The resulting sections were lightly stained with Toluidine Blue and photographed under high magnification (20X objective) using a stereo-microscope. The photographs were then analysed to determine average epidermal cell size (figures 26 and 27).

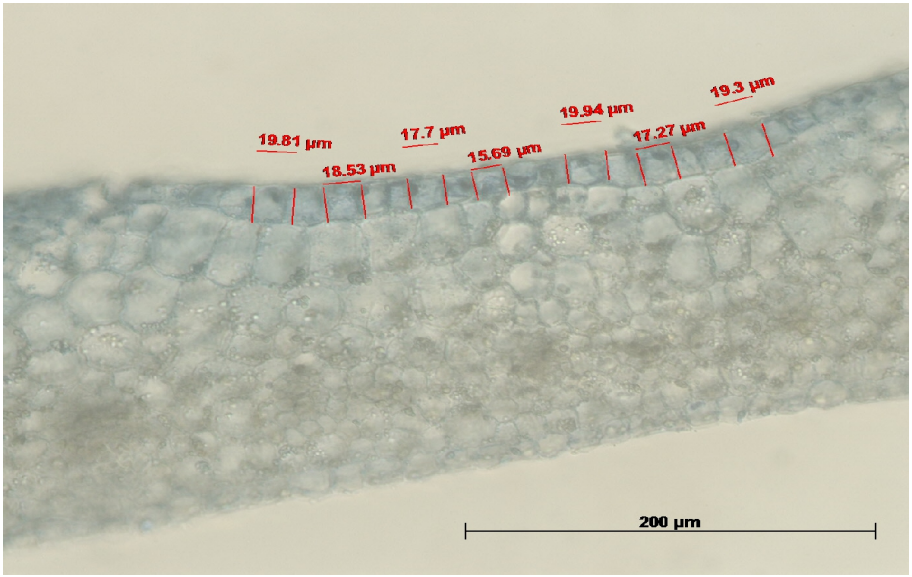

Figure 26. Example of epidermal cell size measurements obtained from cross-section of a 0-3cm ligule-distance leaf sample.

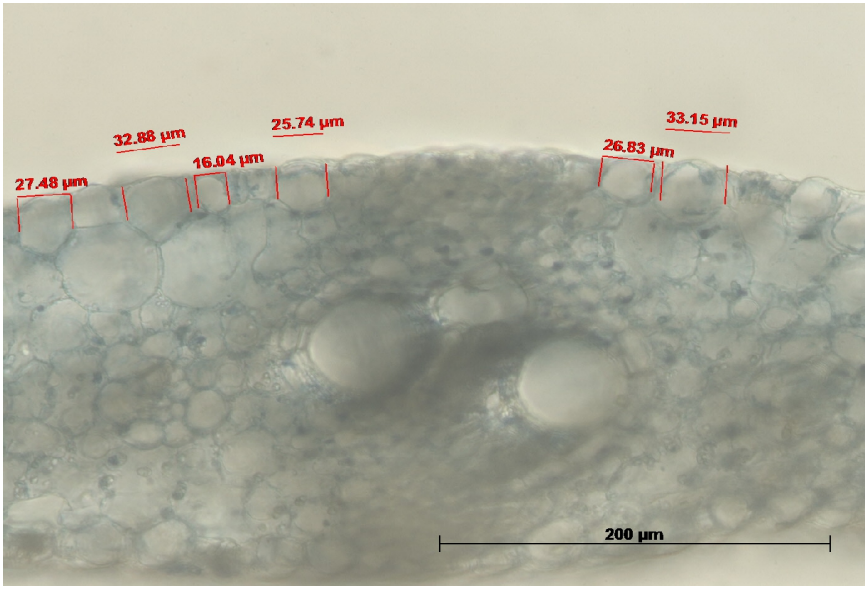

Figure 27. Example of epidermal cell size measurements obtained from a cross-section of a 3-6cm ligule-distance sample.

The measurements obtained from a number of these images were then used to give an average cell size for both sample groups was 16.3um for the 0-3cm samples and 25.8um for the 3-6cm samples. The standard deviations were 2.4 and 5.6um, respectively. A t-test was performed to assess the data. The T-statistic was 6.6, with a p-value of 8.5×10^{-7}. It is thus reasonable to assume that significant differences exist between the average sizes of the two sample groups.

23.3 Hand cryosectioning of plant tissues

Microscopy was carried out using wet-mounted leaf samples, both sectioned and un-sectioned. In general, the thinner leaf samples used in these experiments resulted in a number of samples for which anatomical views were difficult to obtain (figure 28). This was due to the fact that, when the sample is thinner in cross-section than it is possible to slice, it will tend to rest in on its adaxial/abaxial surfaces.

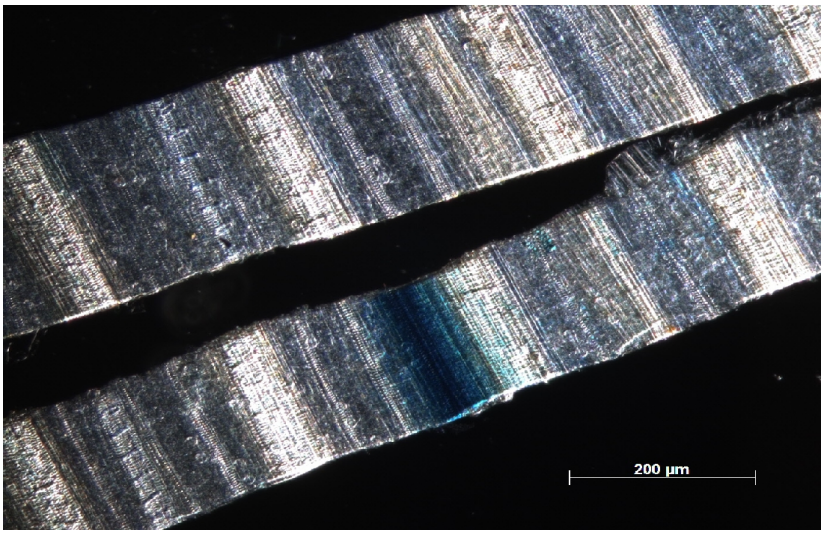

Figure 28. Expressing (blue) and non-expressing leaf sample cross-sections obtained using standard hand-sectioning techniques, viewed along the adaxial surface. Note that the samples themselves are thinner then 200um, as they would otherwise tend to lie at right angles to the image shown.

To solve this problem, hand cryosectioning was performed where standard hand-sectioning approaches did not produce usable slices, or where the tissue had a tendency to tear rather than cleanly cut. The results were very encouraging, as frozen samples tended to shear without bending. This resulting in thin, even slices between 50 and 100um (figure 29), as compared with the 180um slices obtainable by hand. Scalpel blades were found to be superior to razor blades for this technique.

This novel approach proved to be well suited to producing wet-mount samples for analysis under a microscope, as the histological stain produced by X-Gluc staining would be lost when approaches such as resin fixation were used. In addition, the procedure is rapid, easy to perform, and requires not specialised equipment other than low-temperature storage.

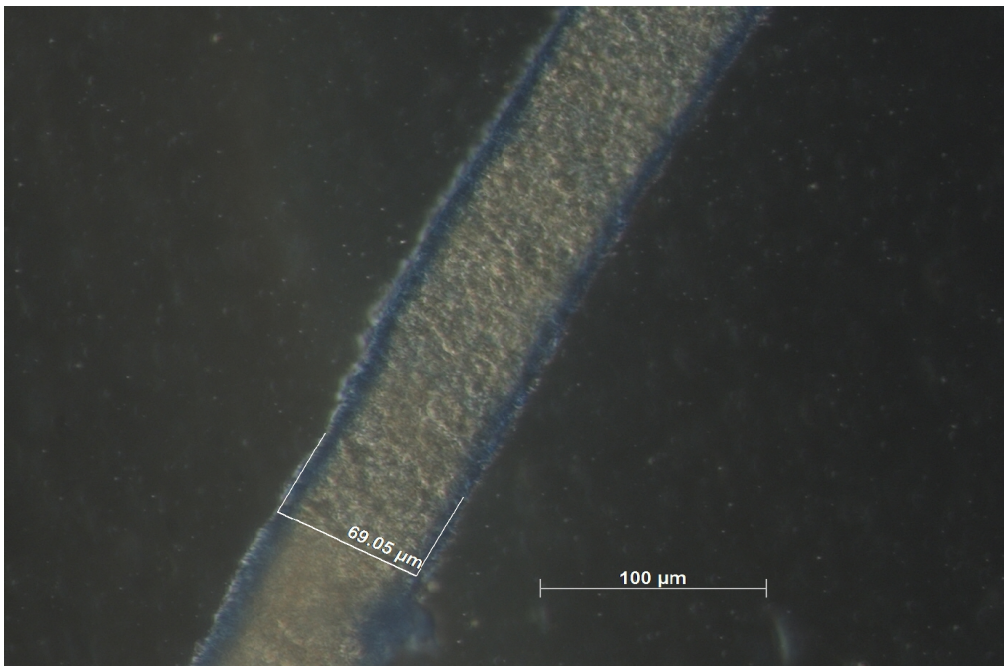

Figure 29. A transverse section of maize leaf sectioned using the hand cryo-sectioning approach, seen from above. Sample is lightly stained with Toluidine Blue, to emphasize the edges of the sectioned tissue.